

## Characteristics of the Re-calculated *Yohkoh*/SXT Temperature Response

A. Takeda

© Springer •••

**Abstract** The temperature response functions of the *Yohkoh*/SXT are re-calculated based on the most recent elemental abundances and ionization balance available in the CHIANTI atomic database version 6.0.1. The new standard responses are calculated for three types of abundances; *i.e.*, ‘coronal’, ‘hybrid’, and ‘photospheric’ abundances included in the CHIANTI database, and are available in SolarSoft since 2010. Comparison plots of the new and old response functions and filter ratios are available at the *Yohkoh* Legacy data Archive (<http://solar.physics.montana.edu/ylegacy>). The three new responses generally peak at higher temperatures (at  $\approx 10$  MK) than the former standard response (at  $\approx 5.6$  MK) based on Mewe’s spectral model. The new responses with coronal and hybrid abundances have higher peak counts by a factor of 3 and 2, respectively, than those with the photospheric abundances and the former response based on Mewe’s model. The correction of the filter ratios depends on the type of filters and the range of the ratios to be used. In the significant cases, the new filter ratio produces 20 to 30% higher temperatures than the previous calibration. The choice of elemental abundance has a strong influence on the derived temperatures and emission measures, and often produces variation significantly larger than the statistical and systematic errors considered so far.

**Keywords:** Corona, Models, Instrumentation and Data Management

### 1. Introduction

The Soft X-ray Telescope (SXT) onboard *Yohkoh*(1991-2001) observed the whole or selected area of the Sun in the X-ray range of 3 to 37 Å(1% peak response of the thinnest analysis filter). The best corrected and value-added products from SXT are maintained and provided by the *Yohkoh* Legacy data Archive (YLA) (Takeda, 2009). The SXT has five X-ray analysis filters designed to perform temperature diagnosis of the observed plasma. The SXT spectral response (spectral sensitivity) and its modification by analysis filters are given as effective areas in Tsuneta *et al.* (1991).

<sup>1</sup> Dept. of Physics, Montana State University  
email: takeda@solar.physics.montana.edu

The SXT temperature response functions (hereafter simply described as response functions) are the expected CCD signals (*i.e.*, the number of electrons produced by incident X-rays) through each analysis filter, assuming the observed plasma is isothermal. As a computational process, the wavelength-dependent effective area functions are convolved with the synthesized solar spectra. The latter are determined by the elemental abundances, ionization balance, and underlying emission models. By the commonly adopted filter-ratio technique, the SXT can provide a fairly reasonable estimate of the mean temperature and emission measure of the large-scale coronal features; *i.e.*, Acton, Weston, and Bruner (1999) computed the expected SXT flux from 25 models of coronal differential emission measures (DEMs) ranging from quiet sun, coronal holes, active regions, and some flares. They showed that 24 of 25 SXT filter ratio temperatures fall within 0.1 (in logarithmic scale) of the mean DEM temperatures of the models. It should be noted that their conclusions may not apply to the highly resolved features, where multi-thermal nature of the plasma is essential, and the DEM would not be as smooth as those used in Acton, Weston, and Bruner (1999).

The SXT response functions were initially generated by J. Lemen based on the solar spectral model by Mewe, Gronenschild, and van den Oord (1985) and Mewe, Lemen, and van den Oord (1986). With minor modifications, these response functions have been used in the standard SXT analysis software throughout the *Yohkoh* mission. Since early 2000s, however, improved atomic data and spectral models have become available from the CHIANTI atomic database for plasma emission in the X-ray range (Dere *et al.*, 2001). Through a series of revisions, CHIANTI has matured to the current version 6.0.1 (Dere *et al.*, 2009) used in the analysis presented here. It is the purpose of this paper to update the SXT response functions based on the latest available database to benefit the general users of the SXT data.

While models of spectral emission and ionization balance are expected to converge with time, the elemental abundances in the corona appear to vary from region to region and with time within a given observed volume. The elemental abundance in the coronal plasma is often described in terms of the first ionization potential (FIP) of the elements. Feldman *et al.* (1992) remarked that low FIP elements ( $\text{FIP} \lesssim 10$  eV) in the average quiet corona are enhanced by about a factor of four relative to their photospheric values. In contrast, Meyer (1985, 1991) concluded that high FIP elements ( $\text{FIP} \gtrsim 10$  eV) are depleted typically by a factor of four in the corona while the low FIP elements remain at their photospheric values. Fludra and Schmelz (1999) proposed a ‘hybrid’ abundance with enhancement of low FIP elements by a factor of 2.1 and the depletion of high FIP elements by a factor of 0.65. From the study of emission lines formed below 1 MK, Feldman *et al.* (1992) reported photospheric abundances observed in some types of phenomena or location, *e.g.*, ejecta of photospheric material, impulsive flares, above sunspots, *etc.* More recently, Feldman and Widing (2002) claimed that the abundances in the corona evolve with the age of the observed region, *i.e.*, newly emerged regions have an abundance close to that of the photosphere but low FIP elements become enhanced with time in the corona. This study is based on XUV spectra formed at temperatures less than 1 MK. Thus knowledge of the coronal abundances for temperatures over 1 MK is still insufficient. In

view of these uncertainties, these new SXT responses are calculated for the following three abundance models, (a) ‘coronal’ abundances by Feldman *et al.* (1992), (b) ‘hybrid’ abundances proposed by Fludra and Schmelz (1999), and (c) ‘photospheric’ abundances by Grevesse and Sauval (1998). Users may choose as appropriate as new understanding emerges.

There are a few published works regarding revised response functions of the SXT. Schmelz *et al.* (1999) investigated the SXT response functions modified by the use of more recent atomic data employed by the SERTS project. They pointed out that the choice of the elemental abundance and ionization balance significantly affects the behavior of the SXT response functions and the temperatures and emission measures derived from them. Shimojo, Hara, and Kano (2002) revised the SXT response functions under CHIANTI version 3.0.3, with the elemental abundance of Feldman *et al.* (1992) and the ionization balance by Mazzotta *et al.* (1998). Since it was a part of the preparatory study for the *Hinode* mission, a revision of the standard *Yohkoh* response and related software was not published.

The YLA’s new response functions introduced herein and the revised software to utilize them, have been distributed since 2010 in SolarSoft (Freeland and Handy, 1998). The trend of the new response functions and influence on the derived temperatures and emission measures are discussed below in comparison with the former results.

## 2. Calculation

The calculation of the new response functions was made with the use of the CHIANTI database and software package, version 6.0.1, included in SolarSoft. Corresponding to the three types of elemental abundances described above, the following three files in the CHIANTI package were used; ‘sun\_coronal\_ext.abund’, ‘sun\_hybrid\_ext.abund’, and ‘sun\_photospheric\_grevesse07.abund’. The ionization balance ‘chianti.ioneq’, introduced in Dere *et al.* (2009), was employed for all three cases. An isothermal plasma with a volume emission measure of  $10^{44}$  cm $^{-3}$  was assumed, as with the former response functions.

The effective area function compiled by N. Nitta in 2006 was adopted for our calculation. It has narrow (0.05 Å), uniform wavelength bins, as required to work with CHIANTI software, and yields only a negligible difference in its spectral behavior from the previous area functions.

It should be noted that the effective areas were treated as temporally constant. Aging or failure of the instruments can generally change their response. It is realized that the failure of the entrance filters, which SXT suffered several times since November 1992, affects the effective area. However, the epoch-dependent sensitivity correction is made in the SXT analysis software when applied to individual cases. Therefore, for this paper, all the differences found among different response functions result exclusively from the solar spectra synthesized in generating each response function.

The new response functions calculated with the use of the (a) coronal, (b) hybrid, and (c) photospheric abundances were compared with the previous results, *i.e.*, (d) the former standard SXT response, and (e) calculation by Shimojo,

**Table 1.** Summary of the SXT response functions calculated or compared in this study. For each function, the label of the function, abundance, ionization balance, and the emission model are given with the reference.

---

(a)	New SXT response with coronal abundance ‘sun_coronal_ext.abund’ (Feldman <i>et al.</i> , 1992) ‘chianti.ioneq’ (Dere <i>et al.</i> , 2009) CHIANTI ver. 6.0.1 (Dere <i>et al.</i> , 2009)
(b)	New SXT response with hybrid abundance ‘sun_hybrid_ext.abund’ (Fludra and Schmelz, 1999) ‘chianti.ioneq’ (Dere <i>et al.</i> , 2009) CHIANTI ver. 6.0.1 (Dere <i>et al.</i> , 2009)
(c)	New SXT response with photospheric abundance ‘sun_photospheric_grevesse07.abund’ (Grevesse and Sauval, 1998) ‘chianti.ioneq’ (Dere <i>et al.</i> , 2009) CHIANTI ver. 6.0.1 (Dere <i>et al.</i> , 2009)
(d)	Former standard SXT response coronal abundance by Meyer (1985) Arnaud and Rothenflug (1985) Mewe, Gronenschild, and van den Oord (1985) and Mewe, Lemen, and van den Oord (1986)
(e)	Shimojo, Hara, and Kano (2002) ‘feldman.abund’ (Feldman <i>et al.</i> , 1992) ‘mazzotta_etal.ioneq’ (Mazzotta <i>et al.</i> , 1998) CHIANTI ver. 3.0.3 (Dere <i>et al.</i> , 2001)
(f)	Reference function 1 ‘meyer_coronal.abund’ (Meyer, 1985) ‘arnaud_rothenflug.ioneq’ (Arnaud and Rothenflug, 1985) CHIANTI ver. 6.0.1 (Dere <i>et al.</i> , 2009)
(g)	Reference function 2 ‘feldman.abund’ (Feldman <i>et al.</i> , 1992) ‘mazzotta_etal.ioneq’ (Mazzotta <i>et al.</i> , 1998) CHIANTI ver. 6.0.1 (Dere <i>et al.</i> , 2009)

---

Hara, and Kano (2002). For the purpose of making clear the source of difference, comparison was made with two more reference functions, *i.e.*, (f) and (g), which use the same abundance and ionization balance pair as (d) and (e), but calculated with CHIANTI version 6.0.1. The information on these response functions is summarized in Table 1.

### 3. Results

#### 3.1. Temperature Response Functions

The upper plot in Figure 1 shows the response functions calculated for the Al/Mg/Mn composite filter (denoted by AlMg hereafter), which was most frequently used throughout the mission. The lower plot is for the Be filter, which is the thickest SXT analysis filter and often used for flare observations. Other X-ray filters have trends similar to the AlMg filter with different peak counts and small shifts of peak temperature depending on the filter transmission.

The AlMg response functions calculated with the CHIANTI models (curves a, b, c, e, f and g) generally peak at a higher temperature (at around 10 MK) than the model by Mewe *et al.* (curve d), which peaks at 5.6 MK, or in a logarithmic scale,  $\log T=6.75$ .

Under the same spectral model, the choice of abundances makes a significant impact on the responses; *e.g.*, the peak counts of the response functions with hybrid (curve b) and photospheric (curve c) abundances are roughly 60% and 30% of that with coronal abundances (curve a). The choice of ionization balance, on the other hand, has less influence; *e.g.*, the ionization balance files compared here (curves a and g) make less than 10% difference. Although the abundance files used in (a) and (g) are not identical either, they do not make much difference since the essential part of the abundances are both based on Feldman *et al.* (1992).

As for the Be filter, the choice of abundances, again, markedly influences the resulting response. While the response curves with Meyer's model (curves d and f) and photospheric (curve c) abundances are monotonically increasing, the CHIANTI coronal abundances (curves a, e, and g) yield a hump at around 15 MK ( $\log T=7.2$ ). Again, the ionization balance has only a minor influence (curves a and g).

It turned out that the emission model also has a considerable effect on the response; for the same abundance and ionization balance pair, the CHIANTI models ver. 3.0.3 and ver. 6.0.1 yield substantial differences in the shape and amplitude of the response curves (see curves e and g). After the ver. 3.0.3, there were repeated update of the line intensities of the ions affecting the soft X-ray spectra, as well as the improvement in the method calculating the continuum intensity (Enrico Landi, private communication). This indicates that the SXT response functions with CHIANTI ver. 6.0.1 is more reliable than those with ver. 3.0.3 and earlier models. Therefore, the choice of abundances turns out to be the major factor affecting the SXT response functions.

#### 3.2. Filter Ratios

The dependence of the filter ratios on abundance and emission model is displayed in Figure 2. The upper panel shows the ratios of the response of the AlMg filter to that of the thin Al filter (denoted by Al.1, following the SXT convention) calculated from the five response functions from Table 1. Because of their greater response to plasma in the 1-4 MK range relative to other filters, these filters are

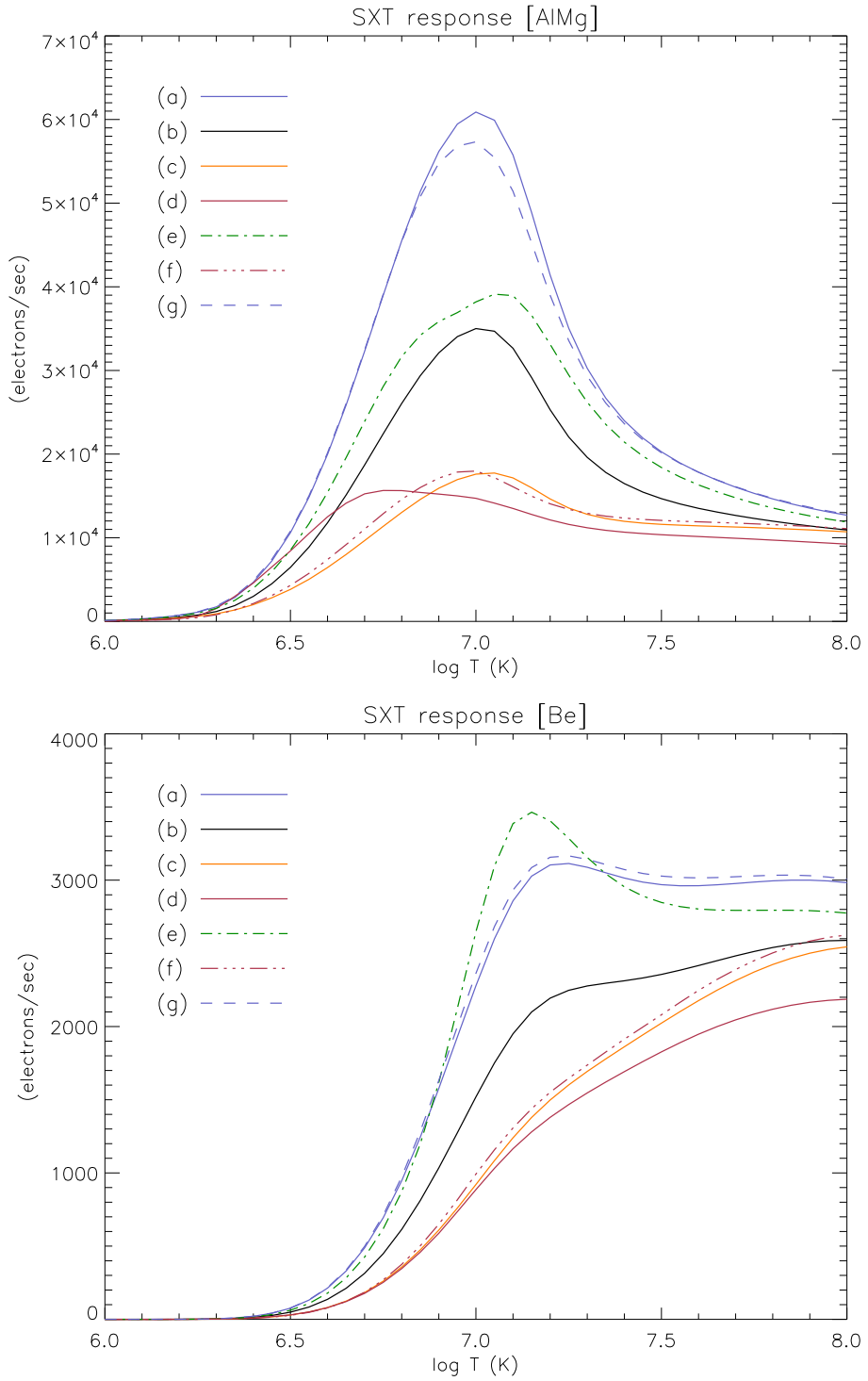


**Figure 1.** SXT response functions for the AlMg (top) and Be (bottom) filters. The symbols, (a) to (g), correspond to the parameters summarized in Table 1.

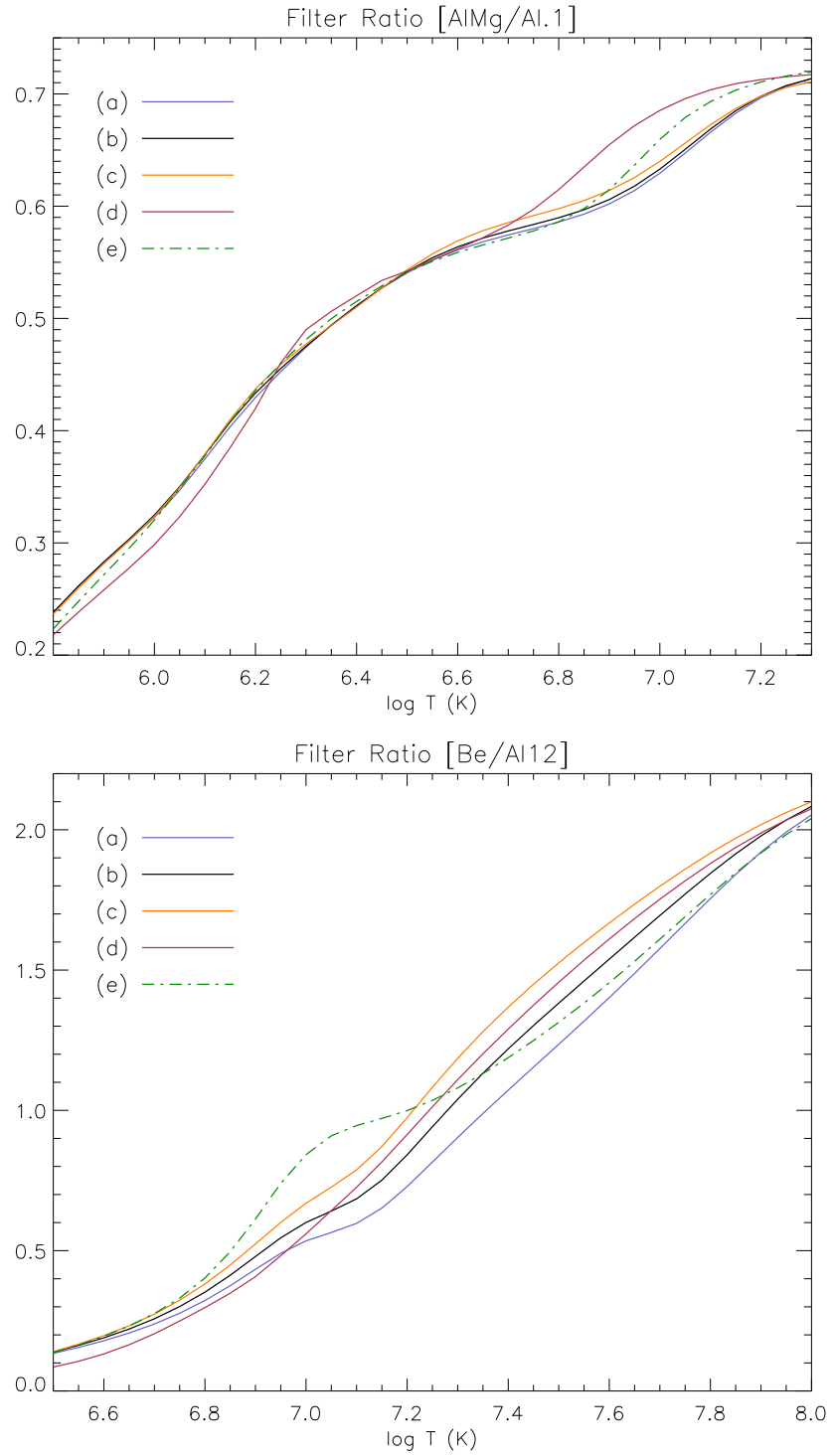


**Figure 2.** SXT filter ratios for the filter pairs, AlMg/Al.1 (top) and Be/Al12 (bottom). The symbols, (a) to (e), correspond to the parameters summarized in Table 1.

typically used for the analysis of non-flaring structures. There is a remarkable separation seen in the filter-ratio curves for the ratios ranging from 0.6 to 0.7, corresponding to the temperature range of the peak of the two response curves. In this range, all three new ratio curves yield higher temperature than the previous calibration (based on Mewe *et al.*, 1985, 1986); *e.g.*, at the ratio of 0.65, the new ratios (curves a, b, and c) yield 40 to 45% higher temperatures than the previous calibration (curve d). For the ratio range less than 0.45, on the contrary, the new ratios result in slightly lower temperatures ( $\approx 10\%$  at the ratio 0.35) than the previous calibration.

The lower panel shows the ratio curves of the Be filter relative to the thick Al filter (denoted by Al12), often used for the analysis of flares. It is notable that for the ratio 0.5 and above, the new ratio with coronal abundances (curve a) yields roughly 30% higher temperature than the previous result (curve d). On the other hand, the ratio from the hybrid abundances (curve b) yields only slightly higher temperature ( $\approx 10\%$  at the ratio of 0.65) than the previous result (curve d). The ratio curve from the photospheric abundances yields lower temperatures than the other new curves and previous result, throughout the range. With the ratios lower than 0.5, all the new curves provide lower temperatures than the previous result (curve d).

As was the case of the former responses based on Mewe, Gronenschild, and van den Oord (1985), five out of ten filter pairs result in a double-valued function and are thus only usable for restricted ratio range for determining temperatures by the simple filter-ratio technique. For the filter pairs which do not yield double-valued ratios for the entire range (*i.e.*, AlMg/Al.1, Be/Al.1, Be/AlMg, Be/Mg, and Be/Al12 filters) the new ratio functions typically yield 20 to 30% higher temperatures than the previous calibration for hot plasma around 10 MK. In this temperature range, the temperatures obtained for a given ratio value are the highest with the coronal abundances, then followed by the hybrid and then photospheric abundances. For plasma cooler than 5 MK, on the other hand, the new curves tend to yield slightly lower temperatures than the previous calibration. The behavior of the new and old ratio curves depends on the filter combination and the ratio range to be used. The details should be examined for individual cases (see YLA documentation for details).

## 4. Discussion

### 4.1. Difference among Response Functions due to Abundances

SXT responses are explained by two components, *i.e.*, emission lines from the ions and continua formed by the electrons. Figure 3 shows the contributions of these components to the new response functions with (a) coronal, (b) hybrid, and (c) photospheric abundances. Regarding the AlMg responses (left panels), the largest line contribution comes from Fe ions (curve ii), with secondary contributions from Mg, Si, and Ni ions (the total contribution from the three elements is shown as curve iii). Since these contributing elements all have low FIP, the abundances of these elements are enhanced about a factor of 4 in the coronal

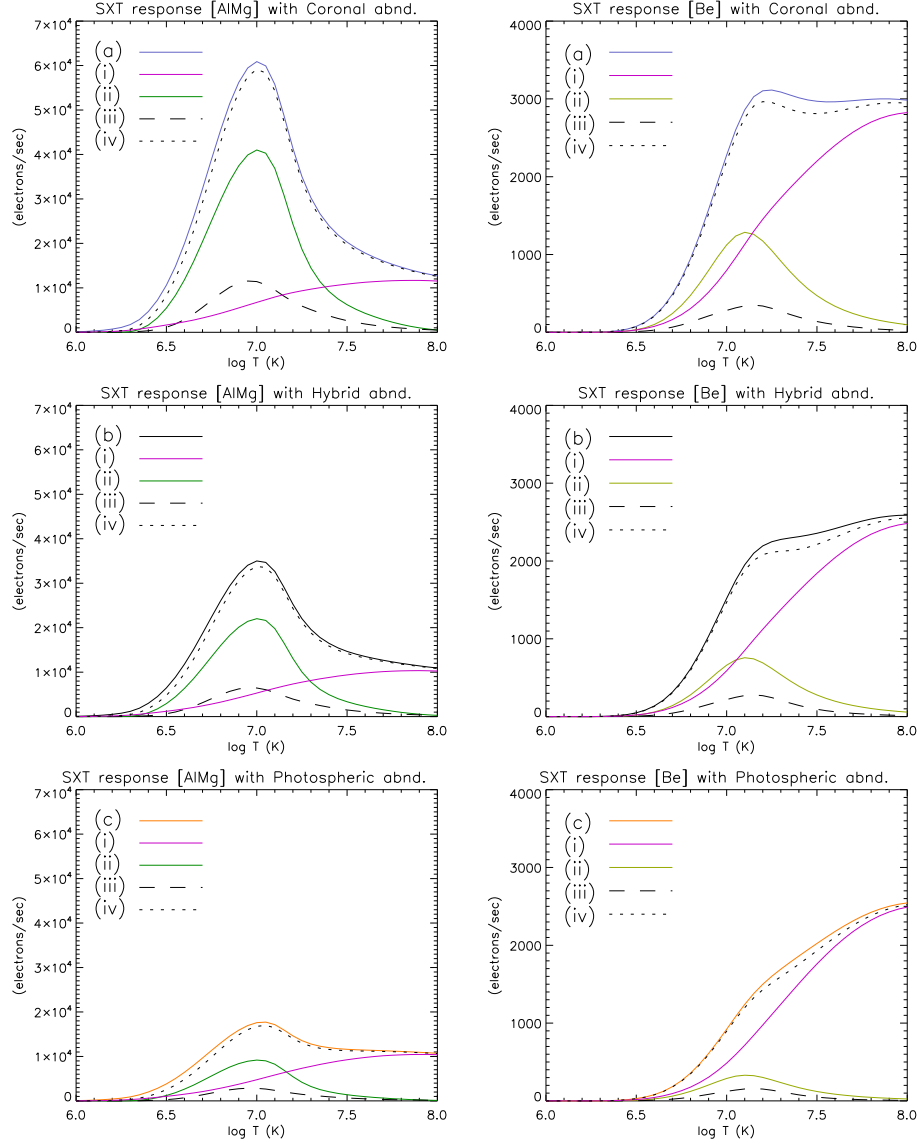


**Figure 3.** Contributions of the continuum and major emission lines to the new SXT response functions with coronal (a, top panels), hybrid (b, middle panels), and photospheric (c, bottom panels) abundances. Left panels: the AlMg filter responses. (i) continuum contribution, *i.e.*, total of free-free, free-bound, and two photon processes, (ii) contributions from Fe ions, (iii) total contributions from Mg, Si, and Ni ions, (iv) sum of (i) through (iii). Right panels: the Be filter responses. (i) same as the above, (ii) contributions from Si ions, (iii) total contributions from Mg, Fe, S, and Ca ions, (iv) same as the above.

abundances and about a factor of 2 in the hybrid abundances relative to the photospheric abundances. This explains the notable difference of the peak counts of the response curves (a), (b) and (c). The continuum component consists of radiations by free-free, free-bound, and two photon processes. The contribution of the continuum is overwhelming at high temperature ( $\log T > 7.4$ ), while it is less significant at lower temperatures, especially in the cases of (a) coronal and (b) hybrid abundances. The majority of electrons are supplied by H and He atoms, and those abundances are kept constant (H) or have little variation (He) among three cases. Therefore, the continuum component shows little difference among the response curves (a), (b) and (c).

In the Be responses (right panels), the continuum is the most dominant component to the total response, and differences due to abundance assumption is not substantial. The most significant line contributor is Si ions, shown as curve (ii) in the right panels. Other large contributions come from the ions, Mg, Fe, S, and Ca, whose total contribution is shown as curve (iii). Again, these are low FIP elements (except S that has medium value, 10.36 eV), and thus the total line contribution significantly varies according to the enhanced abundances of those elements. This enhanced line contribution in (a) coronal and (b) hybrid abundances produces the hump seen at around  $\log T > 7.1$  in the response curves.

The previous standard responses for SXT (curve d in Figure 1) is based on the coronal abundances by Meyer (1985). This set of abundances is characterized by the depletion of high FIP elemental abundances, rather than the enhancement of low FIP elements, relative to their photospheric values. It is therefore reasonable that the peak of curve d is as low as the new response with photospheric abundances (curve c). When recalculated with CHIANTI 6.0.1 emission model (curve f), it behaves similarly to the curve (c) in Figure 1.

#### 4.2. Significance of the Difference of Derived Temperatures and Emission Measures

For a given filter pair, the different versions of filter ratio (among those listed in Table 1) can yield very close temperatures to each other. However, the distinct difference in amplitude of the response functions generally produces substantially different emission measures. As a typical case, the ratio curves for AlMg/Al.1 all give similar temperature around  $\log T = 6.5$  at the filter ratio, 0.54 (see Figure 2). However, the emission measures derived from the new response functions (a), (b), and (c) are a factor of 0.8, 1.3, and 2.2 larger respectively, than the previous result derived from the response curve (d).

The preliminary analysis of a few active regions demonstrates that the difference in temperatures and emission measures resulting from different version of response functions are in general significantly larger than the amount of the estimated uncertainty that includes both statistical (*i.e.*, photon noise) and systematic errors. For the latter, the present standard SXT software only provides errors from the data decompression included in data and calibration (background and stray light) images, which comes to less than 20 % of the statistical errors for the relevant cases. Even with the higher reliability of the latest CHIANTI emission model, the variation resulting from different assumptions of abundances remains a dominant source of uncertainty associated with the filter-ratio method.

### 4.3. Possible Choice of Elemental Abundances

The SXT observations include diverse plasmas with different height and activity levels. The true abundances of the observed corona is naturally expected to differ from any of the three abundances considered in this study. Although it is impossible to know the true abundances, the following suggestion may help in selecting the SXT response function suitable for the observed corona.

The coronal abundances by Feldman *et al.* (1992), which SXT's new response function (a) is based on, were determined for the average quiet corona, where the enhancement of the low-FIP elements is considered to work more effectively than hotter plasma which SXT is most sensitive. Considering the reports by Feldman *et al.* (1992) and Feldman and Widing (2002), the photospheric abundances (the new response function c), may be applicable when the observed plasma is thought to be newly brought from the photosphere (*e.g.*, emerging flux and very young active regions). Abundances during the fast energetic events (intense flares) may also be photospheric, because the high-FIP elements would also be ionized there and it is hard to expect the enhancement of the low-FIP elements persists effectively. For the rest of the cases, *i.e.*, normal active regions and flares, the hybrid abundances by Fludra and Schmelz (1999) (SXT response function b) may serve best.

The hybrid model has therefore been set as the default SXT response function in the YLA and SolarSoft software for SXT temperature analysis. Users also can choose other options (coronal and photospheric abundance as well as the former response functions) by specifying them in a keyword.

## 5. Conclusion

The SXT temperature response functions were re-calculated based on the most recent emission model, elemental abundances, and ionization balance available in the CHIANTI database and software package, version 6.0.1. The new response functions were calculated for three different abundances, *i.e.*, coronal, hybrid, and photospheric abundances, so that users can select as desired.

The new response functions peak near 10 MK, which is hotter than the former standard response based on Mewe *et al.* (1985, 1986). This shift is mainly caused by the application of the CHIANTI emission model. The coronal and hybrid abundances yield higher response counts than the former standard response by a factor of 3 and 2, respectively, while the photospheric abundance yields similar counts to the former response. The choice of abundance significantly affects the amplitude of the response, whereas the ionization balances compared herein are less influential.

The new filter ratios generally yield 10 to 30% higher temperatures than the former standard ratios in the relatively-high temperature range (above 8 MK or  $\log T > 6.9$ ). In contrast, lower temperatures are obtained from the new ratio curves in the relatively-low temperature range. For the Be/Al12 filter pair, the photospheric abundance yields about 10% lower temperatures than the former calibration throughout the ratio range. The new response functions and the

filter-ratio curves in comparison with the previous results are available in the YLA documentation (<http://solar.physics.montana.edu/ylegacy>).

With the understanding that the emission model and the ionization balance are in a considerably matured state, the choice of abundances has the strongest influence on the derived temperatures and emission measures. Their variation due to different choices of abundances are often larger than the estimated amount of SXT statistical plus systematic errors currently taken into account. This implies, without knowledge to determine or narrow the range of abundances of the observed plasma, those variations become a dominant source of uncertainty in calculating the temperatures and emission measures by the filter-ratio method.

**Acknowledgements** The author thanks the YLA team for their steady support of the project, and in particular Loren Acton and David McKenzie for valuable comments and wording advice. The author is grateful to Hugh Hudson (UCB) for careful reading of the manuscript. The author is indebted to Nariaki Nitta (LMSAL) for improving the SXT effective area functions, and to Masumi Shimojo (NAOJ) for providing the response functions of his work in 2002. CHIANTI is a collaborative project involving researchers at NRL (USA), RAL (UK), and the Universities of: Cambridge (UK), George Mason (USA), and Florence (Italy). The author thanks Enrico Landi (Univ. of Michigan) for his prompt response as a chianti\_help contact person. The YLA is supported by NASA as a resident archive, a Heliosphysics Data Environment Enhancement project (NNX09AH64G).

## References

- Acton, L.W., Weston, D.C., Bruner, M.E.: 1999, Deriving solar X ray irradiance from Yohkoh observations. *J. Geophys. Res.* **104**, 14827–14832. doi:10.1029/1999JA900006.
- Arnaud, M., Rothenflug, R.: 1985, An updated evaluation of recombination and ionization rates. *Astron. Astrophys. Suppl.* **60**, 425–457.
- Dere, K.P., Landi, E., Young, P.R., Del Zanna, G.: 2001, CHIANTI-An atomic database for emission lines. IV. Extension to X-ray wavelengths. *Astrophys. J. Suppl.* **134**, 331–354. doi:10.1086/320854.
- Dere, K.P., Landi, E., Young, P.R., Del Zanna, G., Landini, M., Mason, H.E.: 2009, CHIANTI - An atomic database for emission lines. IX. Ionization rates, recombination rates, ionization equilibria for the elements hydrogen through zinc and updated atomic data. *Astron. Astrophys.* **498**, 915–929. doi:10.1051/0004-6361/200911712.
- Feldman, U., Widing, K.G.: 2002, A review of the first ionization potential effect on elemental abundances in the solar corona and in flares. *Phys. Plasmas* **9**, 629–635. doi:10.1063/1.1435000.
- Feldman, U., Mandelbaum, P., Seely, J.F., Doschek, G.A., Gursky, H.: 1992, The potential for plasma diagnostics from stellar extreme-ultraviolet observations. *Astrophys. J. Suppl.* **81**, 387–408. doi:10.1086/191698.
- Fludra, A., Schmelz, J.T.: 1999, The absolute coronal abundances of sulfur, calcium, and iron from Yohkoh-BCS flare spectra. *Astron. Astrophys.* **348**, 286–294.
- Freeland, S.L., Handy, B.N.: 1998, Data analysis with the SolarSoft system. *Solar Phys.* **182**, 497–500.
- Greveste, N., Sauval, A.J.: 1998, Standard solar composition. *Space Sci. Rev.* **85**, 161–174. doi:10.1023/A:1005038224881.
- Mazzotta, P., Mazzitelli, G., Colafrancesco, S., Vittorio, N.: 1998, Ionization balance for optically thin plasmas: Rate coefficients for all atoms and ions of the elements H to NI. *Astron. Astrophys. Suppl.* **133**, 403–409. doi:10.1051/aas:1998330.
- Mewe, R., Gronenschild, E.H.B.M., van den Oord, G.H.J.: 1985, Calculated X-radiation from optically thin plasmas. V. *Astron. Astrophys. Suppl.* **62**, 197–254.
- Mewe, R., Lemen, J.R., van den Oord, G.H.J.: 1986, Calculated X-radiation from optically thin plasmas. VI - Improved calculations for continuum emission and approximation formulae for nonrelativistic average Gaunt factors. *Astron. Astrophys. Suppl.* **65**, 511–536.

- Meyer, J.: 1985, Solar-stellar outer atmospheres and energetic particles, and galactic cosmic rays. *Astrophys. J. Suppl.* **57**, 173–204. doi:10.1086/191001.
- Meyer, J.: 1991, Diagnostic methods for coronal abundances. *Advances in Space Research* **11**, 269–280. doi:10.1016/0273-1177(91)90120-9.
- Schmelz, J.T., Saba, J.L.R., Strong, K.T., Winter, H.D., Brosius, J.W.: 1999, Emission measure distribution for an active region using coordinated SERTS and YOHKOH SXT observations. *Astrophys. J.* **523**, 432–443. doi:10.1086/307736.
- Shimojo, M., Hara, H., Kano, R.: 2002, The temperature analysis of Yohkoh/SXT data using the CHIANTI spectral database. In: Martens, P. C. H., Cauffman, D. (eds.) *Multi-Wavelength Observations of Coronal Structure and Dynamics, Cospar Colloquia Series* **13**, 419–420.
- Takeda, A.: 2009, Resident archive services of the Yohkoh Legacy data Archive. *Data Science J.* **8**, IGY1–IGY5.
- Tsuneta, S., Acton, L., Bruner, M., Lemen, J., Brown, W., Caravalho, R., Catura, R., Freeland, S., Jurcevich, B., Owens, J.: 1991, The soft X-ray telescope for the SOLAR-A mission. *Solar Phys.* **136**, 37–67. doi:10.1007/BF00151694.

